

Innovative Modified of Cu-Al/C (C = Biochar, Graphite) Composites for Removal of Procion Red from Aqueous Solution

Alfan Wijaya¹, Patimah Mega Syah Bahar Nur Siregar², Aldi Priambodo¹, Neza Rahayu Palapa^{1,3}, Tarmizi Taher⁴, Aldes Lesbani^{1,3*}

¹Research Center of Inorganic Materials and Complexes, Faculty of Mathematics and Natural Sciences, Universitas Sriwijaya, Palembang, 30139, Indonesia

²Magister Programme Graduate School of Mathematics and Natural Sciences, Universitas Sriwijaya, Palembang, 30139, Indonesia

³Graduate School, Faculty of Mathematics and Natural Sciences, Universitas Sriwijaya, Palembang, 30139, Indonesia

⁴Department of Environmental Engineering, Institut Teknologi Sumatera, Lampung Selatan, 35365, Indonesia

*Corresponding author: aldeslesbani@pps.unsri.ac.id

Abstract

Innovative modification of Cu-Al/C composites was synthesized by coprecipitation method at pH 10 and added biochar (BC) and graphite (GF) to form Cu-Al/BC and Cu-Al/GF composites. Pristine and composites were characterized by XRD, FT-IR, Thermalgravimetric, and surface area using the BET method. The XRD diffraction and FTIR spectrum of Cu-Al/BC and Cu-Al/GF showed that the composite material from LDH, biochar, and graphite was successfully prepared. Modified LDH were surface area higher than the pristine, which obtained 200.90 m²/g and 18.83 m²/g for Cu-Al/BC and Cu-Al/GF respectively. Cu-Al/BC and Cu-Al/GF were tested for selectivity on several anionic dyes, it was known that procion red (PR) dye was more easily adsorbed than other anionic dyes. Materials were applied as adsorbents of procion red (PR) dye. The advantages of composites were evaluated by the regeneration process of adsorbent on PR. The result of composite toward PR re-adsorption process showed that Cu-Al/BC and Cu-Al/GF had structural stability higher than starting materials until five cycles process. Furthermore, materials were applied as adsorbents of procion red (PR) dye. The maximum adsorption capacity obtained was 93.458 mg/g for Cu-Al/BC and 49.505 mg/g for Cu-Al/GF. Both innovative modified composites have shown effective adsorbents to the removal of PR from an aqueous solution.

Keywords

Composites, Adsorption, Procion Red Dye, Selectivity, Structural Stability

Received: 27 April 2021, Accepted: 17 July 2021

<https://doi.org/10.26554/sti.2021.6.4.228-234>

1. INTRODUCTION

Synthetic dyes have become widely used due to their being more durable, more colorful, low cost, and easy to apply on domestic and industrial scales (Lellis et al., 2019). The increasing use of synthetic dyes can create several disadvantages not only for the environment but also for human health. The wastewater of synthetic dyes is an organic pollutant that is difficult to degrade by nature (Eltaweil et al., 2020). One of the synthetic dyes that are intensively used in industrial applications is procion red (PR) (Hua et al., 2020). The structure of PR is shown in Figure 1.

Toxicity of PR thus removal of PR was vital. Various methods to remove dyes wastewater such as photocatalytic degradation (Kumar and Rao, 2017; Natarajan et al., 2020), biological treatment (Tang et al., 2020; Sarkar et al., 2017), coagulation (Mcyotto et al., 2021; Demissie et al., 2021), and adsorption (Palapa et al., 2018; Palapa et al., 2020a; Siregar et al., 2021) have been tested. Adsorption is a method that is widely used

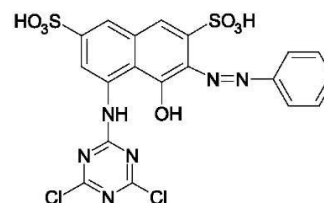


Figure 1. Chemical Structure of Procion Red (PR)

to remove dyes due more efficient, fast process, and cheap (Eltaweil et al., 2020). Many adsorbents can be used to absorb dyes such as kaolin (Mustapha et al., 2019), activated carbon (Quesada et al., 2020; Streit et al., 2019), bentonite (Mohammad et al., 2020), chitosan (Shi et al., 2020), and LDH (layered double hydroxide) (Palapa et al., 2019; Zhao et al., 2017; Palapa et al., 2020b; Siregar et al., 2021; Normah et al., 2021; Juleanti et al., 2021). Layered double hydroxide (LDH)

has high ion exchange and adsorption ability making LDH an appropriate adsorbent for adsorption of various pollutants. LDH has a granular structure and a less stable structure. These properties make the limitation of LDH an adsorbent, especially for the reusability process.

Research conducted by Palapa et al. (2018) using Ni/Al and Zn/Al LDHs to adsorb direct yellow dye showed the efficient process of adsorption. Cu/Al LDH was applied to adsorb malachite green dye with also efficient results (Palapa et al., 2020b). Zn/Fe and Zn/Al were used as efficient adsorbents to adsorb direct yellow dye (Palapa et al., 2019), and Mg/Al LDH to adsorb methylene blue dye (Zhao et al., 2017). All results showed that LDH has a limitation as adsorbent for reuse process, thus modification of LDH is needed to enhance the ability of LDH for dyes adsorption. By modification of LDH through impregnation by carbon-based materials can create the structure stability and performance of LDH. One of the potential carbon materials for LDH support is biochar (BC) and graphite (GF).

Composite of Cu-Al/BC was prepared as adsorbent of malachite green produce an adsorption capacity of 108.96 mg/L (Palapa et al., 2020b). Mg/Al-BC composite was also successfully used as an adsorbent of malachite green with an adsorption capacity of 70.922 mg/g (Badri et al., 2021) and Mg/Al-Carbon Dot composite was synthesized to adsorb methylene blue with an adsorption capacity of 185 mg/g (Zhang et al., 2014). In this research, Cu-Al/BC and Cu-Al/GF composites are prepared, used as adsorbents, and tested for selectivity on several anionic dyes to know which dyes are more easily adsorbed. The adsorption parameters to be studied in this study include adsorption isotherms and adsorption thermodynamics which are calculated using the Langmuir and Freundlich equation. The stability of composites is evaluated by regeneration of adsorbent until five cycles adsorption process.

2. EXPERIMENTAL SECTION

2.1 Chemicals and Instrumentation

The chemicals used in the experiment were $\text{Cu}(\text{NO}_3)_2 \cdot 3\text{H}_2\text{O}$ by EMSURE® ACS, $\text{Al}(\text{NO}_3)_3 \cdot 9\text{H}_2\text{O}$ by Sigma Aldrich, NaOH by EMSURE® ACS, rice husk was obtained from Bukata Organic®, Indonesia, fabricant graphite from Sigma Aldrich and water was demineralized using Purite® water purification apparatus. Pristine and composites were characterized by XRD, FTIR, and BET. Analysis XRD was performed by Rigaku Miniflex-6000 diffractometer. FT-IR characterization using FT-IR Shimadzu Prestige-21. Analysis BET using Quantachrome Micrometric ASAP. The concentration of PR was analyzed using Spectrophotometer Ultra Violet-Visible Biobase BK-UV 1800 PC at a wavelength of 545 nm.

2.2 Preparation of Cu/Al LDH

Synthesis of Cu/Al LDH was conducted as a similar procedure by Palapa et al. (2020b) using the coprecipitation method at pH 10. The synthesis of Cu/Al LDH was carried out in the following procedure: as much as 100 mL of $\text{Cu}(\text{NO}_3)_2 \cdot 3\text{H}_2\text{O}$

0.75 M was mixed with 100 mL $\text{Al}(\text{NO}_3)_3 \cdot 9\text{H}_2\text{O}$ 0.25 M (3:1) in a beaker. The reaction was stirred until homogeneous mixtures then 50 mL NaOH 2 M was added until pH 10. The mixture was stirred for 20 hours. The solid precipitate was then filtered, washed and dried at 110°C for 120 minutes.

2.3 Preparation of Cu-Al/BC and Cu-Al/GF

Cu-Al/BC and Cu-Al/GF Composites were prepared using the coprecipitation method in the following procedure: as much as 10 mL $\text{Cu}(\text{NO}_3)_2 \cdot 3\text{H}_2\text{O}$ 0.75 M mixed with 10 mL $\text{Al}(\text{NO}_3)_3 \cdot 9\text{H}_2\text{O}$ 0.25 M and stirred for 60 minutes until homogeneous. The resulting mixture was added with 1 g of (BC or GF) while stirring and added with NaOH 2 M until pH 10. The mixed solution was stirred for 3 days at a temperature of 80 °C. The composites were filtered, washed and dried at 40 °C for 120 minutes.

2.4 Selectivity of Anionic Dye Mixtures

The selectivity of anionic dye mixtures was carried out to find the most widely absorbed anionic dyes in each adsorbent by mixing anionic dyes of congo red (CR), procion red (PR), methyl orange (MO) and methyl red (MR) with the same concentration, then added adsorbents and stirred with a time variation of 15, 30, 60, 90, and 120 minutes, then measured absorbance at the wavelength of each dye.

2.5 Desorption and Regeneration of Adsorbent

The desorption process was carried out to test the adsorbent efficiency for the reuse of the adsorbent. In this study, the desorption process was used as an ultrasonic process. The desorption process was carried out using 50 mL of PR. As much as 50 mg/L was added with 1 g of adsorbent and stirred for 120 minutes. Then, dry the used adsorbent and take 0.01 g, add 10 mL of water to the ultrasonic process. The regeneration process using the adsorbent that has been used is as follows: 50 mL of PR at 50 mg/L was stirred for 120 minutes and solution was measured using a UV-Vis Spectrophotometer at 545 nm. The dried adsorbent was then used again for the desorption process, successively. The adsorbent was applied until five cycles adsorption process with the same procedure as the initial run.

2.6 Adsorption Process

The adsorption process of PR was studied through the influence of the initial concentration of PR and adsorption temperature. The variation of initial concentration of PR and temperature adsorption was carried out with the concentration of CR (60, 70, 80, 90 and 100) mg/L, 0.02 g of adsorbent and 20 mL of PR, then stirred for 100 minutes with a variation of the adsorption temperature at 30, 40, 50, and 60 °C. The concentration of the PR was measured by UV-Vis spectrophotometer at 545 nm. Thermodynamic parameters were obtained from the Langmuir and Freundlich equations. Langmuir is assumed to be a chemical and monolayer adsorption process, while Freundlich is assumed to be a physical and multilayer adsorption

process. Isotherm Langmuir and Freundlich's equations are according to previous works of literature (Palapa et al., 2020b).

3. RESULTS AND DISCUSSION

Diffractogram of Cu/Al LDH, BC, GF and composites are shown in Figure 2. Cu/Al LDH materials have typical peaks with good crystallinity with diffraction angles at 11.6° (003), 23.5° (006), 34.3° (101), 35.1° (012), 37.8° (104), 39.8° (015), 44.4° (107), 47.3° (018) and 61.4° (110/113) indicated that the formation of the Cu/Al LDH structure was following the JCPDS 46-0099 file. Figure 2b showed that broad peak the presence of high carbon content on BC with diffraction at 22.30° (002). The diffraction patterns of GF as shown in Figure 2c, material has good crystallinity with diffraction at 26.4° (002). The diffraction patterns of Cu-Al/BC as shown in Figure 2d resemble the diffraction patterns of Cu/Al LDH and biochar. The Cu-Al/BC composite material has an amorphous diffraction pattern due to the characteristics of biochar with a diffraction peak of around 23° . The diffraction pattern in Cu-Al/GF as shown in Figure 2e resemble that of Cu/Al LDH and graphite. Cu-Al/GF composite material is shown in Figure 2e which shows that there are typical peaks of Cu/Al LDH and graphite. According to Kusrimi et al. (2019) Cu-Al/GF composite material has a distinctive diffraction pattern of graphite around 26.54° (002) with sharp peaks.

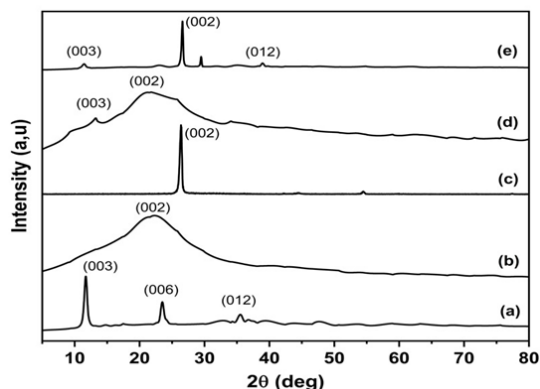


Figure 2. XRD Powder Patterns of Cu/Al LDH (a), BC (b), GF (c), Cu-Al/BC (d), and Cu-Al/GF (e)

Nitrogen adsorption-desorption analysis on Cu/Al LDH, BC, GF and Cu-Al/BC and Cu-Al/GF composites is shown in Figure 3. Figure 3 shows that the nitrogen adsorption pathway is not the same as the nitrogen desorption pathway which indicates that the material has hysteresis. The hysteresis that occurs in the graph shows the pores in the material. The pattern in Figure 3 shows that the materials in Cu/Al LDH, BC, GF, Cu-Al/BC and Cu-Al/GF composites follow type IV isotherms. Type IV isotherm shows hysteresis of mesoporous sized materials with strong hysteresis activity on the adsorbent-adsorbate interaction.

Table 1 showed that Cu-Al/BC had surface area four-fold than pristine LDH and BC. The results of the BET analysis

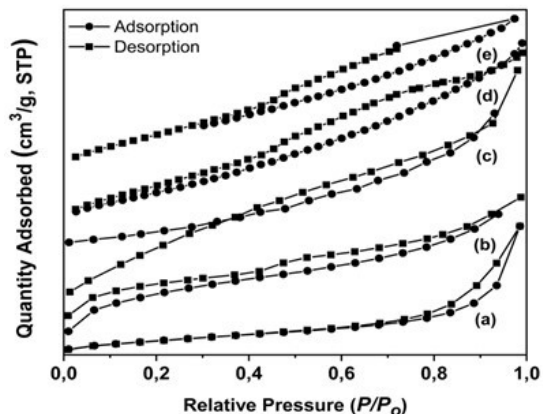


Figure 3. BET profile of Cu-Al LDH (a), BC (b), GF (c), Cu-Al/BC (d), and Cu-Al/GF (e)

showed that the starting material had an increase in surface area after the formation of composites which obtained 200.90 and $18.83 \text{ m}^2/\text{g}$ for Cu-Al/BC and Cu-Al/GF respectively. This shows that the synthesis process has been successful.

Table 1. BET Analysis of Materials

Materials	Surface Area (m^2/g)	Pore Size (nm), BJH	Pore Volume (cm^3/g), BJH
Cu-Al LDH	46.279	10.393	0.116
BC	50.936	12.089	0.025
GF	9.394	3.169	0.027
Cu-Al/BC	200.90	7.03	0.350
Cu-Al/GF	18.83	3.132	0.046

Figure 4a shows the FTIR spectrum of Cu/Al LDH had vibrations at 3448 cm^{-1} which indicates the presence of O-H stretching, 1635 cm^{-1} presence of O-H bending, 1381 cm^{-1} presence of N-O stretching, 794 cm^{-1} presence of Al-O and 462 cm^{-1} presence of Zn-O and Cu-O. The FTIR spectrum of BC and Cu-Al/BC as shown in Figures 4b and 4d had vibrations that indicate the presence of O-H stretching, C-H bending, O-H bending, and C-O stretching. The FTIR spectrum of GF and Cu-Al/GF as shown in Figures 4c and 4e had vibrations presence of O-H stretching, vibrations at 2368 cm^{-1} presence of C-H, O-H bending, N-O, Zn-O and Cu-O. Composites of Cu-Al/BC and Cu-Al/GF had all vibrations of Cu-Al LDH, BC, and GF as a result of two components were involved in the composites.

Figure 5 showed the thermal analysis of materials. The thermogravimetry of Cu/Al LDH patterns had only an exothermic phase because Cu/Al LDH consists of inorganic components. The exothermic peak of Cu/Al LDH was attributed to the decomposition of water at around 110°C , decomposition of a layer at around 650°C , and loss of anions on interlayer at around $200\text{-}300^\circ \text{C}$. BC had organic content thus endothermic

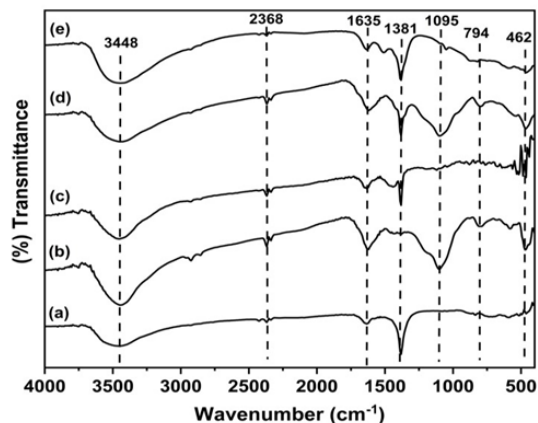


Figure 4. FTIR Spectrum of Cu/Al LDH (a), BC (b), GF (c), Cu-Al/BC (d), and Cu-Al/GF (e)

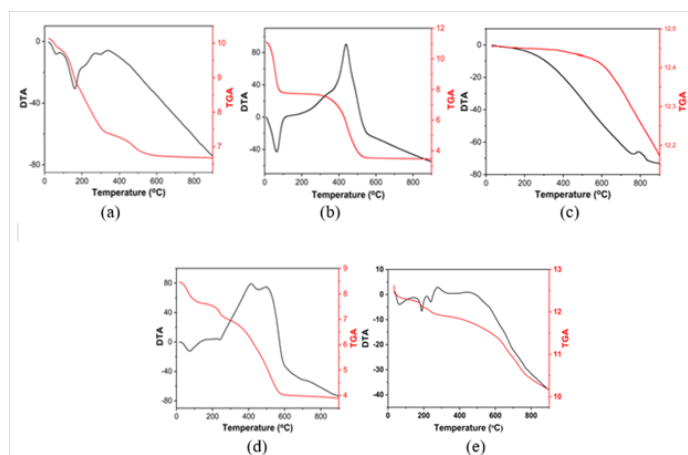


Figure 5. Thermal Profile of Cu/Al LDH (a), BC (b), GF (c), Cu-Al/BC (d), and Cu-Al/GF (e)

mic peak was found due to oxidation of organic parts around 490 °C. GF has only one decomposition peak at 760 °C. This decomposition peak was denoted that GF was pure without other ingredients, including water. Cu-Al/BC and Cu-Al/GF composites had organic and inorganic components thus had two kinds of endothermic and exothermic peaks.

Table 2 shows the adsorption concentration of each dye in the selectivity of anionic dye mixtures. Based on the data in Table 2, the concentration of PR adsorption is greater compared to other dyes. This suggests that PR is more easily to adsorption process using Cu-Al/BC and Cu-Al/GF adsorbents. The results of the regeneration of each adsorbent on the PR dye can be seen in Figure 6. As an equal result of increasing surface area properties after the formation of composite Cu-Al/BC thus adsorption of PR was higher than starting materials. Starting materials of Cu/Al LDH had a less stable structure so modifications of composites based on carbon materials such as BC and GF to produce a stable structure that can be reused

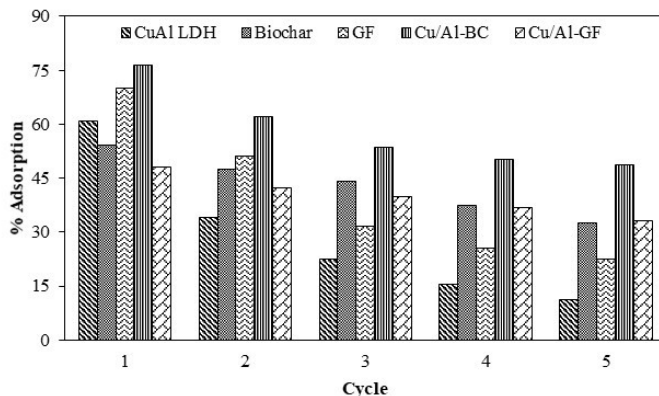


Figure 6. Regeneration of Adsorbents

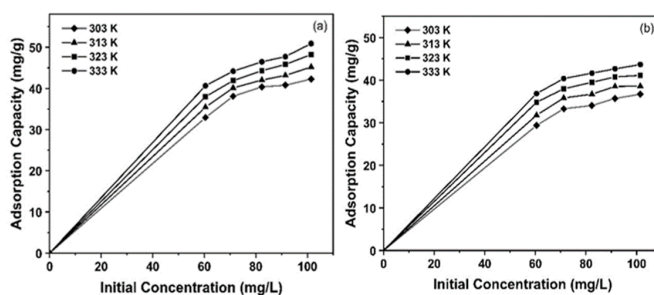


Figure 7. Effect of Initial Concentration of PR and Adsorption Temperature on Cu-Al/BC (a) and Cu-Al/GF (b)

on the adsorption process. The result of the composites regeneration process on PR showed that Cu-Al/BC and Cu-Al/GF had structural stability higher than starting materials. Effect of initial concentration of PR and adsorption temperature on Cu-Al-BC and Cu-Al/GF as shown in Figure 7. Increasing the adsorption temperature will increase the adsorption capacity.

Table 3 presents the isotherm adsorption parameters, which identifies that the Langmuir model is better than the Freundlich model. The Langmuir model indicates the adsorption process is a monolayer. Table 3 showed that the maximum adsorption capacity of Cu-Al/BC is larger than other materials that so it has high effectivity on CR adsorption. Table 4 showed the thermodynamic adsorption of CR. The ΔH had positive values indicated that adsorption occurs endothermally which requires an energy of adsorption process. The value of ΔG was more negative with increasing temperature indicated that adsorption on all materials was spontaneous. The value of ΔS indicated the degree of irregularity. The positive value of ΔS indicates that an increase in irregularity on the surface. In Table 5, Cu-Al/BC and Cu-Al/GF composites had the highest adsorption capacity than several adsorbents. Thus materials were effective adsorbents to the removal of PR from aqueous solution.

Table 2. Selectivity of Anionic Dye Mixtures

Adsorbents	Times (Minutes)	Concentration Adsorption (mg/L)			
		MR	MO	PR	CR
Cu-Al/BC	0	0.000	0.000	0.000	0.000
	15	0.672	0.095	1.519	0.476
	30	3.507	0.587	8.228	1.349
	60	5.149	1.591	15.063	3.492
	90	5.821	2.008	25.443	5.556
	120	6.791	2.140	36.203	7.619
Cu-Al/GF	0	0.000	0.000	0.000	0.000
	15	0.597	0.303	0.127	0.317
	30	0.896	1.420	7.848	1.190
	60	2.836	1.591	10.000	3.095
	90	4.179	1.818	11.772	3.413
	120	5.746	1.837	13.418	3.651

Table 3. Isotherm Adsorption

Adsorbents	Adsorption Isotherm	Adsorption Constant	T (°C)			
			30	40	50	60
Cu-Al/BC	Langmuir	Qmax	53.476	63.291	81.301	93.458
		kL	0.066	0.074	0.081	0.106
		R ²	0.984	0.995	0.998	0.995
	Freundlich	n	3.425	3.667	3.801	4.507
		kF	13.107	15.160	16.939	21.023
		R ²	0.845	0.929	0.984	0.977
Cu-Al/GF	Langmuir	Qmax	46.296	46.512	47.393	49.505
		kL	0.060	0.084	0.114	0.132
		R ²	0.992	0.992	0.999	0.999
	Freundlich	n	3.576	4.216	5.157	5.596
		kF	11.564	14.800	18.897	21.340
		R ²	0.911	0.871	0.941	0.936

Table 4. Thermodynamic Adsorption

Adsorbents	T (K)	Qe (mg/g)	ΔH (kJ/mol)	ΔS (J/mol.K)	ΔG (kJ/mol)
Cu-Al/BC	303	32.911	15.041	0.051	-0.423
	313	35.443			-0.934
	323	37.975			-1.444
	333	40.633			-1.955
Cu-Al/GF	303	29.367	14.327	0.047	0.157
	313	31.772			-0.311
	323	34.810			-0.779
	333	36.835			-1.246

Table 5. Adsorption of PR by Several Adsorbents

Materials	Adsorption Capacity (mg/g)	References
Corncob Activated Carbon	2.86	(Nazifa et al., 2018)
Spent Tea Leaves	3.28	(Heraldy et al., 2016)
Waste Fe (III)/Cr (III) Hydroxide	3.28	(Namasivayam and Sumithra, 2006)
Agricultural Wastes	6.12	(Nor et al., 2015)
Raw and Acid-Treated Montmorillonite K10	11.04	(Sarma et al., 2018)
<i>Luffa cylindrica</i>	13.9	(Oliveira et al., 2011)
Cornstalk	15.9	(Valencia et al., 2001)
Sewage Sludge Ash (SSA)	28.82	(Hu and Hu, 2014)
Cu-Al/BC	93.458	This Research
Cu-Al/GF	49.505	This Research

4. CONCLUSIONS

Innovative modification of Cu-Al/BC and Cu-Al/GF composites was successfully formed. The surface area properties of Cu-Al/BC and Cu-Al/GF were larger than starting materials, which obtained 200.90 m²/g and 18.83 m²/g respectively. Based on the selectivity test for anionic dye mixtures, it is known that PR is more easily adsorbed than other anionic dyes. Cu-Al/BC and Cu-Al/GF composites were high structural stability on PR re-adsorption process until five cycles process. The maximum adsorption capacity obtained was 93.458 mg/g for Cu-Al/BC and 49.505 mg/g for Cu-Al/GF. Thus, Cu-Al/BC and Cu-Al/GF can be used as an effective adsorbents to removal of PR from aqueous solution.

5. ACKNOWLEDGEMENT

Authors are acknowledgement to Universitas Sriwijaya through Hibah Profesi 2021 for this financial research by contract No. 0014/UN9/SK.LP2M.PT/2021. Special thanks to Research Center of Inorganic Materials and Complexes FMIPA Universitas Sriwijaya for laboratory analysis.

REFERENCES

- Badri, A. F., P. M. S. B. N. Siregar, N. R. Palapa, R. Mohadi, M. Mardiyanto, and A. Lesbani (2021). Mg-Al/Biochar Composite with Stable Structure for Malachite Green Adsorption from Aqueous Solutions. *Bulletin of Chemical Reaction Engineering and Catalysis*, **16**(1); 149–160
- Demissie, H., G. An, R. Jiao, T. Ritigala, S. Lu, and D. Wang (2021). Modification of high content nanocluster-based coagulation for rapid removal of dye from water and the mechanism. *Separation and Purification Technology*, **259**; 117845
- Eltaweil, A., H. A. Mohamed, E. M. Abd El-Monaem, and G. El-Subruiti (2020). Mesoporous magnetic biochar composite for enhanced adsorption of malachite green dye: Characterization, adsorption kinetics, thermodynamics and isotherms. *Advanced Powder Technology*, **31**(3); 1253–1263
- Heraldy, E., R. R. Osa, and V. Suryanti (2016). Adsorption of Procion Red MX 8B using spent tea leaves as adsorbent. *AIP Conference Proceedings*, **1710**(1); 30025
- Hu, S.-H. and S.-C. Hu (2014). Application of magnetically modified sewage sludge ash (SSA) in ionic dye adsorption. *Journal of the Air and Waste Management Association*, **64**(2); 141–149
- Hua, P., L. Sellaoui, D. Franco, M. S. Netto, G. L. Dotto, A. Bajahzar, H. Belmabrouk, A. Bonilla-Petriciolet, and Z. Li (2020). Adsorption of acid green and procion red on a magnetic geopolymer based adsorbent: Experiments, characterization and theoretical treatment. *Chemical Engineering Journal*, **383**; 123113
- Juleanti, N., N. R. Palapa, T. Taher, N. Hidayati, B. I. Putri, and A. Lesbani (2021). The Capability of Biochar-Based CaAl and MgAl Composite Materials as Adsorbent for Removal Cr(VI) in Aqueous Solution. *Science and Technology Indonesia*, **6**(3); 196–203
- Kumar, S. G. and K. K. Rao (2017). Comparison of modification strategies towards enhanced charge carrier separation and photocatalytic degradation activity of metal oxide semiconductors (TiO₂, WO₃ and ZnO). *Applied Surface Science*, **391**; 124–148
- Kusrini, E., A. Suhrowati, A. Usman, M. Khalil, and V. Degirmenci (2019). Synthesis and characterization of graphite oxide, graphene oxide and reduced graphene oxide from graphite waste using modified Hummers's method and zinc as reducing agent. *Synthesis*, **10**(6); 1093–1104
- Lellis, B., C. Z. Fávoro-Polonio, J. A. Pamphile, and J. C. Polonio (2019). Effects of textile dyes on health and the environment and bioremediation potential of living organisms. *Biotechnology Research and Innovation*, **3**(2); 275–290
- Mcyotto, F., Q. Wei, D. K. Macharia, M. Huang, C. Shen, and C. W. Chow (2021). Effect of dye structure on color removal efficiency by coagulation. *Chemical Engineering Journal*, **405**; 126674
- Mohammad, S., I. Suzylawati, et al. (2020). Study of the adsorption/desorption of MB dye solution using bentonite adsorbent coating. *Journal of Water Process Engineering*, **34**;

- 101155
- Mustapha, S., M. Ndamitso, A. Abdulkareem, J. Tijani, A. Mohammed, and D. Shuaib (2019). Potential of using kaolin as a natural adsorbent for the removal of pollutants from tannery wastewater. *Heliyon*, **5**(11); 2923
- Namasivayam, C. and S. Sumithra (2006). Adsorption of anionic dyes on to waste Fe (III)/Cr (III). *Journal of Environmental Science and Engineering*, **48**(1); 69–74
- Natarajan, S., V. Anitha, G. P. Gajula, and V. Thiagarajan (2020). Synthesis and characterization of magnetic super-adsorbent Fe_3O_4 -PEG-Mg-Al-LDH nanocomposites for ultrahigh removal of organic dyes. *ACS Omega*, **5**(7); 3181–3193
- Nazifa, T. H., N. Habba, A. Aris, and T. Hadibarata (2018). Adsorption of Procion Red MX-5B and Crystal Violet Dyes from Aqueous Solution onto Corncob Activated Carbon. *Journal of the Chinese Chemical Society*, **65**(2); 259–270
- Nor, N. M., T. Hadibarata, Z. Yusop, and Z. M. Lazim (2015). Removal of brilliant green and procionred dyes from aqueous solution by adsorption using selected agricultural wastes. *Jurnal Teknologi*, **74**(11); 11
- Normah, N. R. Palapa, T. Taher, R. Mohadi, H. P. Utami, and A. Lesbani (2021). The Ability of Composite Ni/Al-carbon based Material Toward Readsorption of Iron(II) in Aqueous Solution. *Science and Technology Indonesia*, **6**(3); 156–165
- Oliveira, E., S. Montanher, and M. Rollemberg (2011). Removal of textile dyes by sorption on low-cost sorbents. A case study: sorption of reactive dyes onto *Luffa cylindrica*. *Desalination and Water Treatment*, **25**(1-3); 54–64
- Palapa, N. R., N. Juleanti, N. Normah, T. Taher, and A. Lesbani (2020a). Unique adsorption properties of malachite green on interlayer space of Cu-Al and Cu-Al-SiW₁₂O₄₀ layered double hydroxides. *Bulletin of Chemical Reaction Engineering and Catalysis*, **15**(3); 653–661
- Palapa, N. R., R. Mohadi, and A. Lesbani (2018). Adsorption of direct yellow dye from aqueous solution by Ni/Al and Zn/Al layered double hydroxides. *AIP Conference Proceedings*, **2026**(1); 20018
- Palapa, N. R., B. R. Rahayu, T. Taher, A. Lesbani, and R. Mohadi (2019). Kinetic Adsorption of Direct Yellow Onto Zn/Al and Zn/Fe Layered Double Hydroxides. *Science and Technology Indonesia*, **4**(4); 101–104
- Palapa, N. R., T. Taher, B. R. Rahayu, R. Mohadi, A. Rachmat, and A. Lesbani (2020b). CuAl LDH/Rice husk biochar composite for enhanced adsorptive removal of cationic dye from aqueous solution. *Bulletin of Chemical Reaction Engineering and Catalysis*, **15**(2); 525–537
- Quesada, H. B., T. P. de Araujo, D. T. Vareschini, M. A. S. D. de Barros, R. G. Gomes, and R. Bergamasco (2020). Chitosan, alginate and other macromolecules as activated carbon immobilizing agents: a review on composite adsorbents for the removal of water contaminants. *International Journal of Biological Macromolecules*, **164**; 2535–2549
- Sarkar, S., A. Banerjee, U. Halder, R. Biswas, and R. Bandyopadhyay (2017). Degradation of synthetic azo dyes of textile industry: a sustainable approach using microbial enzymes. *Water Conservation Science and Engineering*, **2**(4); 121–131
- Sarma, G. K., S. SenGupta, and K. G. Bhattacharyya (2018). Adsorption of monoazo dyes (Crocein Orange G and Procion Red MX5B) from water using raw and acid-treated montmorillonite K10: insight into kinetics, isotherm, and thermodynamic parameters. *Water, Air, and Soil Pollution*, **229**(10); 1–17
- Shi, Q.-X., Y. Li, L. Wang, J. Wang, and Y.-L. Cao (2020). Preparation of supported chitosan adsorbent with high adsorption capacity for Titan Yellow removal. *International Journal of Biological Macromolecules*, **152**; 449–455
- Siregar, P. M. S. B. N., N. R. Palapa, A. Wijaya, E. S. Fitri, and A. Lesbani (2021). Structural stability of Ni/Al layered double hydroxide supported on graphite and biochar toward adsorption of congo red. *Science and Technology Indonesia*, **6**(2); 85–95
- Streit, A. F., L. N. Côrtes, S. P. Druzian, M. Godinho, G. C. Collazzo, D. Perondi, and G. L. Dotto (2019). Development of high quality activated carbon from biological sludge and its application for dyes removal from aqueous solutions. *Science of The Total Environment*, **660**; 277–287
- Tang, R., Y. Wang, S. Yuan, W. Wang, Z. Yue, X. Zhan, and Z.-H. Hu (2020). Organoarsenic feed additives in biological wastewater treatment processes: Removal, biotransformation, and associated impacts. *Journal of Hazardous Materials*; 124789
- Valencia, S., M. Pascua, J. Movillon, and H. Braza (2001). Adsorption of basic rhodamine red, basic methylene blue, reactive procion red, and reactive procion blue textile dyes by cornstalk. *Philippine Agricultural Scientist (Philippines)*, **84**(3); 304–312
- Zhang, M., Q. Yao, C. Lu, Z. Li, and W. Wang (2014). Layered double hydroxide-carbon dot composite: high-performance adsorbent for removal of anionic organic dye. *ACS Applied Materials and Interfaces*, **6**(22); 20225–20233
- Zhao, J., Q. Huang, M. Liu, Y. Dai, J. Chen, H. Huang, Y. Wen, X. Zhu, X. Zhang, and Y. Wei (2017). Synthesis of functionalized MgAl-layered double hydroxides via modified mussel inspired chemistry and their application in organic dye adsorption. *Journal of Colloid and Interface Science*, **505**; 168–177